

Chapter 5

Strong Hydrogen Bonds - Protonated Water Clusters and the Hydroxide Monohydrate Anion

In this chapter, the results on the IRMPD spectroscopy of protonated water clusters and of the hydroxide monohydrate anion are presented. The first section focuses on the Zundel cation $H_5O_2^+$ and the partially and totally deuterated species. The structures of larger systems formed by addition of up to two H_2O molecules are studied as well. The last section focuses on the $H_3O_2^-$ anion. Comparison with theory and with recent IRMPD experiments performed on $H_5O_2^+$ at the CLIO laser facility in France^{96,97} and VPD measurements on $H_xO_y^+ \cdot Ar$ ⁹⁸ ($x = 5,7,9$ and $y = 2,3,4$) and $H_3O_2^- \cdot Ar$ ^{97,99} are presented as well. The results on the Zundel cation and the deuterium substituted complexes are published.^{100,101} Additionally, results on larger protonated water clusters and on $H_3O_2^-$ are presented in this chapter.

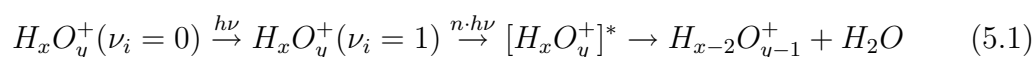
5.1 Gas Phase IRMPD Spectra of Protonated Water Clusters

$H_5O_2^+$ and $H_9O_4^+$ were proposed based on molecular dynamics simulations as limiting structures in the proton transfer process.¹⁴ These two structures were also proposed as release groups in the proton pump process of bacteriorhodopsin.^{15,17} IR studies on hydrated protons in liquid water reveal a quasi-continuum absorption,¹⁰² which makes the assignment of specific bands to $H_5O_2^+$ or $H_9O_4^+$ difficult. Hydrogen bonds are sensitive to perturbations,¹⁰³ hence their study in the gas phase, without the

influence of the environment, is advantageous. Furthermore, the spectral evolution of the proton vibrations as water molecules are stepwise added to the hydronium ion can be studied.

5.1.1 Experiment

The protonated water cluster cations were produced in an electro-spray source and transported through a 100 μm diameter orifice into a vacuum chamber. The ions were mass-selected and then accumulated and trapped at a temperature of less than 100 K . Through collisions with the helium atoms, the cations were cooled in few microseconds to the ambient temperature. This should reduce the contribution of the vibrational hot bands and energetically low-lying isomers to the infrared spectrum. The ions were irradiated by the FELIX pulses, with a macropulse energy in the range from 20 to 40 mJ and a duration of 5 μs . The bandwidth of the FELIX pulse (FWHM) was 0.5 % of the central frequency. The laser was focused in the trap through a 5 mm thick KBr window by a KBr lens with a 479 mm focal length. The IRMPD spectra were recorded by monitoring the fragment ion signals as a function of the laser frequency. Generally, it is considered that the transition between the first two vibrational levels is one-photon followed by multiphoton absorptions and IVR leading to photodissociation:



Here h is the Planck's constant, ν_i represents the vibrational quantum number of the i th vibrational mode and n is the total number of absorbed photons (in this experiment the number of absorbed photons was at least 6 to 18 over the scanning range). At the high FELIX pulse energies the first absorption step might be in some cases two-photon. After irradiation, the parent and fragment ions are extracted from the trap, mass selected and detected.

5.1.2 H_5O_2^+ / $\text{D}_x\text{H}_{5-x}\text{O}_2^+$ ($x = 1 \cdots 5$) Cations

The IR spectrum of the gas phase protonated water cation H_5O_2^+ (referred to as the Zundel cation) was previously measured in the free $O - H$ stretching region ($> 3500 \text{ cm}^{-1}$) by multiphoton photodissociation spectroscopy.¹⁰⁴ The experiments indicate a $\text{H}_2\text{O} \cdots \text{H}^+ \cdots \text{OH}_2$ structure with the proton located symmetrically between the two oxygen atoms of the water ligands. Electronic structure cal-

culations^{105,106} support the experimentally predicted C_2 symmetry geometry (see the inset of Figure 5.1).

The IR spectrum of the Zundel cation in the region of the fundamental vibrations of the central proton, below 2000 cm^{-1} was extensively studied theoretically at different levels of theory.^{8,107-111} These studies indicate that the potential energy surface which describes the motion of the central proton is very flat. Strong anharmonic coupling between the vibrational modes involving the H -atom asymmetric stretch and the outer water molecules are predicted.¹¹¹ Due to the anharmonic coupling of the vibrational modes already at low excitation energies and the high dimension of the system, the theoretical description of the infrared spectrum is challenging.

The Zundel cation has a high dissociation energy ($H_5O_2^+ \rightarrow H_3O^+ + H_2O$) of 31.6 kcal/mol (1.37 eV),¹¹² thus $H_5O_2^+$ is a good model system for the study of strong hydrogen bond systems. No measurements of the infrared spectrum of the Zundel cation were performed in the region of the central proton fundamental vibrations (below 2000 cm^{-1}) previous to the experiments presented here. The fundamental vibrations in this region are important for the understanding of the proton transfer in bulk.

Results

The IRMPD spectrum of the $H_5O_2^+$ cation is shown in Figure 5.1 (upper trace). The spectrum reveals four main bands, labeled b to e , with maxima at 921 , 1043 , 1317 and 1741 cm^{-1} . An additional weak feature denoted with a is observed at 788 cm^{-1} . The observed bands are much wider ($> 100\text{ cm}^{-1}$) than the laser bandwidth which was 5 cm^{-1} at $10\text{ }\mu\text{m}$. Additional features are observed for the high intensity bands b to e . The features corresponding to bands b and c are separated by 30 cm^{-1} from each other and for band d by 70 cm^{-1} . The positions of all observed peaks are listed in Table 5.1.

The IRMPD spectra of the deuterated ions $D_xH_{5-x}O_2^+$ ($x = 0, 1 \dots 5$) were recorded as well (see Figure 5.1 and 5.2). The spectrum of the fully substituted $D_5O_2^+$ ion is shown in the lower trace in Figure 5.1. The spectrum comprises four intense bands at 697 , 795 , 960 and 1296 cm^{-1} labeled from b' to e' , which are slightly narrower than the bands in the $H_5O_2^+$ spectrum and have less pronounced structure. The relative intensities are different from the intensities in the IRMPD spectrum of the $H_5O_2^+$ cation. The four bands b' to e' are red shifted upon $H - D$ substitution with isotope shifts of 1.32 ($b-b'$), 1.31 ($c-c'$), 1.37 ($d-d'$), and 1.34 ($e-e'$). Here it is assumed that peaks with similar labels in the two systems originate from the same transition.

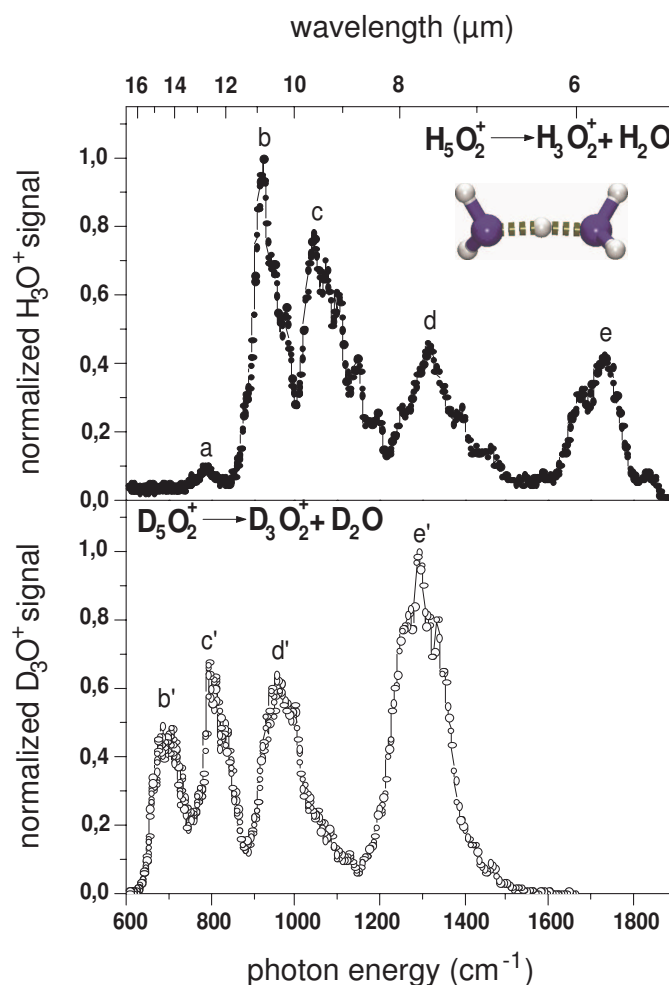


Figure 5.1: IRMPD spectra of the Zundel cation $H_5O_2^+$ (closed circles) and of the deuterated ion $D_5O_2^+$ (open circles). The inset of the upper trace shows the structure of the $H_5O_2^+$ cation.¹⁰⁰ (O - blue spheres, H - white spheres, the dashed line represents the hydrogen bond.)

Similar to $H_5O_2^+$, the width of the absorption bands in the $D_5O_2^+$ spectrum is much larger than the FELIX bandwidth and presents additional structure, which could be an indication of hot band structure. However, their contribution should be reduced significantly by cooling prior dissociation. The zero-point motion of the central proton has a high amplitude leading to an exploration of an unusually large area of the potential energy surface.¹¹¹ This could cause additional structure in the spectrum. Also, multiple photon transitions in which two or more photons are resonant with one vibrational level may be possible. This possibility has been already indicated in the case of $BrHBr^-/BrDBr^-$ and $BrHI^-/BrDI^-$ anions⁷⁵ (see Chapter 4). The multiple photon transitions would appear shifted from single photon transitions due to the

anharmonicity of the potential. Consequently, a negative anharmonicity might lead to multiple photon transitions, which contribute to the high energy tails of bands *b* and *c* in Figure 5.1 (e.g., peaks located at 947, 975, 1071, 1100, 1145 and 1195 cm^{-1}). These features cannot arise from rotational transitions since their structure is different than it would be expected for a nearly prolate top system.

Table 5.1: Experimental band positions for $H_5O_2^+$ and $D_5O_2^+$ and isotope effects (H/D shifts) determined from IRMPD spectra. The position of the band maximum is underlined.

$H_5O_2^+$ band	Frequency cm^{-1}	$D_5O_2^+$ band	Frequency cm^{-1}	H-D shift
a	<u>788</u>			
b	888, <u>921</u> , 947, 975	b'	<u>697</u>	1.32
c	<u>1043</u> , 1071, 1100, 1145, 1195	c'	<u>795</u>	1.31
d	1252, <u>1317</u> , 1390, 1460	d'	<u>960</u>	1.37
e	1687, <u>1741</u> , 1850	e'	<u>1296</u>	1.34

Figure 5.2 shows the IRMPD spectra of the partially deuterated cations. For comparison, the spectra of $H_5O_2^+$ and $D_5O_2^+$ are shown as well. The spectra were recorded with 0.1 μm steps. Broad bands are observed. Different dissociation channels leading to formation of H_3O^+ , DH_2O^+ and other fragments are observed after the irradiation with the laser beam of each partially deuterated ion. Identical spectra are observed for all fragments. This indicates an efficient H/D scrambling during the sequential absorption mechanism, where the ions can absorb photons during the complete duration of a FEL macropulse (5 μs). If the internal rotation is faster than the dissociation lifetime, complete H/D scrambling occurs before dissociation. Since different isotopomers are present in the trap, the infrared spectra of the partially deuterated ions are more complex. However, some features can still be deciphered. The band at $\approx 1500\text{ }cm^{-1}$ which appears only in the mixed spectra, increases with the degree of deuteration for the partially deuterated cations and disappears for $D_5O_2^+$. The band at $\approx 1300\text{ }cm^{-1}$ increases as well with the degree of deuteration and reaches the highest intensity for $D_5O_2^+$. The region between 800 and 1150 cm^{-1} reveals a broad band which might cover additional unresolved peaks. One more band is observed at 770 cm^{-1} in $DH_4O_2^+$ spectrum which increase in intensity and is red shifted to 700 cm^{-1} for $D_5O_2^+$.

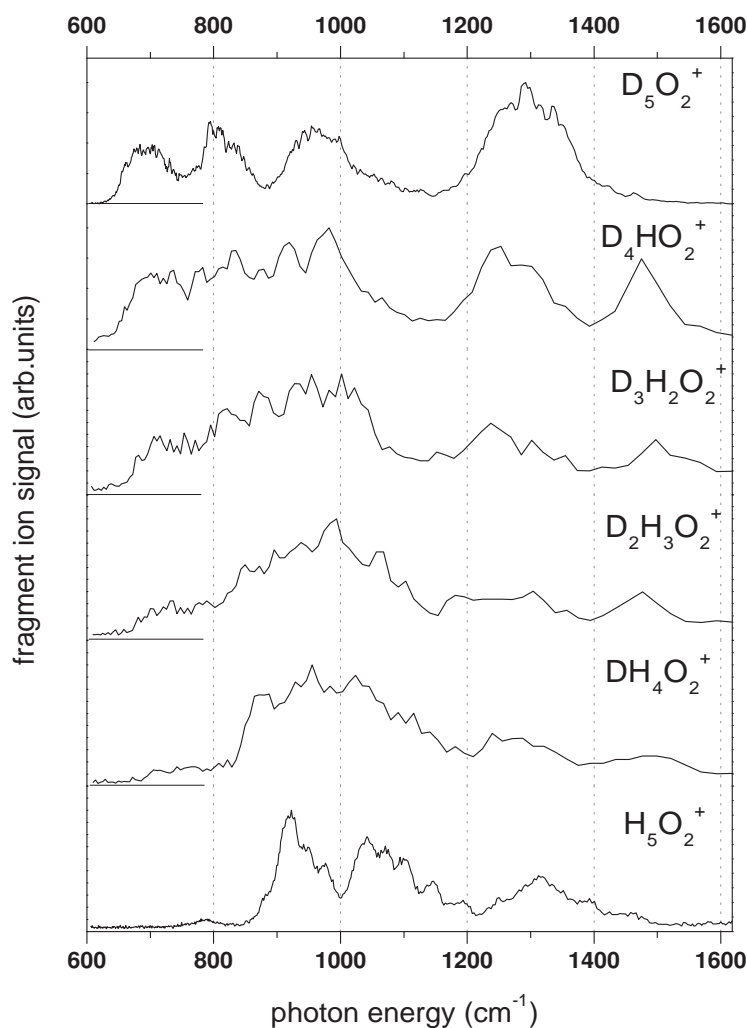


Figure 5.2: IRMPD spectra of the deuterated isotopomers $D_xH_{5-x}O_2^+$ ($x = 0, 1 \dots 5$). For comparison the IRMPD spectra of $D_5O_2^+$ (the most upper panel) and $H_5O_2^+$ (the lowest panel) are shown.¹⁰¹

Discussion

Many scientists simulated the IR spectrum of $H_5O_2^+$ by using a series of different methods¹⁰⁷⁻¹¹¹ and based on these tried to assign the experimentally observed features. The calculations indicated that the harmonic approximation describes well the vibrational modes which involve the terminal water molecules.^{109,113} These include the $H-O-H$ rock, wag, and twist below 600 cm^{-1} , the $H-O-H$ bend at approximately 1750 cm^{-1} and the $O-H$ stretch above 3600 cm^{-1} . Thus, band *e* positioned at 1741 cm^{-1} in Figure 5.1 is assigned to the asymmetric bending vibration of the

water monomers. The B-CCD(T)/TZ2P^a predicted value is 1787 cm^{-1} .¹⁰⁶

The predictions of the central proton vibrational frequencies are more complicated and different levels of theory predict the central proton motions to different frequencies over a broad range. The simulations of the vibrational spectrum of $H_5O_2^+$ in the fingerprint region are very challenging due to the large number of strongly coupled degrees of freedom and of the floppy nature of the central proton. Thus, calculations beyond the harmonic approximation are needed for an adequate description of these vibrations.

Vener *et al.*¹⁰⁹ performed 4D calculations on $H_5O_2^+$. Based on these theoretical studies a tentative assignment to the experimental bands below 1700 cm^{-1} was proposed in our publication.¹⁰⁰ The theoretically predicted frequencies are listed in Table 5.2. According to these calculations, the band *d* located at 1317 cm^{-1} was tentatively assigned to the asymmetric stretch and bands *b* and *c* located at 921 and 1043 cm^{-1} were attributed to the two bending vibrations of the $O \cdots H^+ \cdots O$ moiety.

More recently, higher level calculations were performed by Dai *et al.*¹¹¹ Two of these calculations are mentioned here, the fully coupled 4D (FC 4D) and the full dimensional VCI^b (15D VCI) calculations. In the FC 4D calculations the two bending modes and the asymmetric stretch of the central proton and the symmetric stretch of the two oxygen atoms are involved. The 15D VCI and FC 4D calculations were performed by Dai *et al.*¹¹¹ on the OSS3(p) potential energy surface.¹⁰⁷

Table 5.2: Proposed mode assignments and calculated frequencies at different levels of theory for $H_5O_2^+$.

Mode	Calculations			
	4D ¹ cm^{-1}	FC 4D ² cm^{-1}	15D VCI ² cm^{-1}	MC ³ cm^{-1}
ν_6 ($O \cdots H^+ \cdots O$ sym. str.)	587	571	569	516
ν_7 ($O \cdots H^+ \cdots O$ asym. str.)	1158	1185	902	737/870
ν_8 ($O \cdots H^+ \cdots O$ <i>x</i> bend)	968	1328	1354	
ν_9 ($O \cdots H^+ \cdots O$ <i>y</i> bend)	1026	1344	1388	
ν_{11} H-O-H asym. bend		1860	1788	

¹ Ref.;¹⁰⁹ ² Ref.;¹¹¹ ³ Ref.¹¹⁴

The FC 4D and the 15D VCI calculations predict similar frequencies for the bending modes of the shared proton and the $O \cdots O$ stretch (see Table 5.2). Differences are

^aBrueckner coupled cluster doubles method with a perturbational triple-excitation correction. TZ2P represents the triple- ζ plus double polarization basis set

^bVCI - configuration interaction (CI) calculations using a basis determined from vibrational self-consistent field Hamiltonian

encountered when the frequency of the asymmetric stretch is calculated (1185 cm^{-1} FC 4D value vs. 902 cm^{-1} 15D VCI value). This indicates a stronger coupling between the asymmetric stretch of the central proton and the asymmetric bending vibrations of the water monomers than between the bending vibration of the $O \cdots H^+ \cdots O$ moiety and the asymmetric bending vibrations of the water monomers. This coupling is caused by the central proton motion between the two O atoms in which one water monomer "evolves" to H_3O^+ while the more distant water molecule "evolves" to H_2O .¹¹¹ The FC 4D and 15D VCI methods predict the same ordering of the modes, which is different from the 4D calculations of Vener *et al.*¹⁰⁹ presented above (see Table 5.2). Thus, the asymmetric stretch of the central proton ν_7 is predicted to a lower frequency (902 cm^{-1}) than the bending $O \cdots H^+ \cdots O$ motions ν_8 and ν_9 (\approx 1350 cm^{-1}) (see Table 5.2). A disadvantage of these calculations is a poor description of the $O - H$ monomer stretches.

15D Monte Carlo simulations¹¹⁴ using the OSS3(p) potential energy are the most recently performed full-dimensional calculations. The order of the bands is similar to the 15D VCI calculations, but red shifted up to 80 cm^{-1} . For the asymmetric stretch two vibrations were predicted with strong central proton intensity at even lower frequencies than in the 15D VCI calculations, at 737 and 870 cm^{-1} . Better results than the 15D VCI calculations are obtained for the vibrations of the outer water ligands, however the $O - H$ region is still poorly described. The OSS3(p) surface overestimates the harmonic values for the $O - H$ vibrations. The harmonic values are 3796 and 3700 cm^{-1} which are larger than the experimental values 3609 and 3684 cm^{-1} of the symmetric and the asymmetric stretches, respectively.

The presented full dimensional calculations predict the asymmetric stretch of the central proton at low frequencies, around 900 cm^{-1} . The predicted values are close to the band *b* located at 921 cm^{-1} in the FELIX IRMPD spectrum. The 15D VCI and the 4D FC calculations predict the two bands involving the bending mode of the shared proton close to band *d* positioned at \approx 1300 cm^{-1} . Band *c* located at 1043 cm^{-1} is predicted to a combination of the water dimer wag and the $O \cdots O$ stretch and not to a fundamental transition.

The complexity of the infrared spectrum of the Zundel cation motivated other scientists to perform measurements, either by repeating the IRMPD spectrum⁹⁶ at the free electron laser CLIO situated in France or by measuring the predissociation spectrum of $H_5O_2^+ \cdot Ar$ ^{97,98} (see Table 5.3). These spectra are shown in Figure 5.3, together with the IRMPD spectrum measured at the FELIX facility. The spectrum of the $H_5O_2^+$ cation measured at CLIO⁹⁶ scanned the region from 700 to 1950 cm^{-1} .

Four peaks are observed similar to the IRMPD spectrum measured at FELIX.¹⁰⁰ The peaks present shifts relative to the FELIX bands of 15 to 120 cm^{-1} . For the first two bands, the spectrum measured at CLIO shows maxima where the spectrum measured at FELIX has minima. These strong shifts are surprising and cannot be explained solely by a difference in the ions temperature. The relative intensities are also different in this spectrum compared to the one measured at FELIX.¹⁰⁰

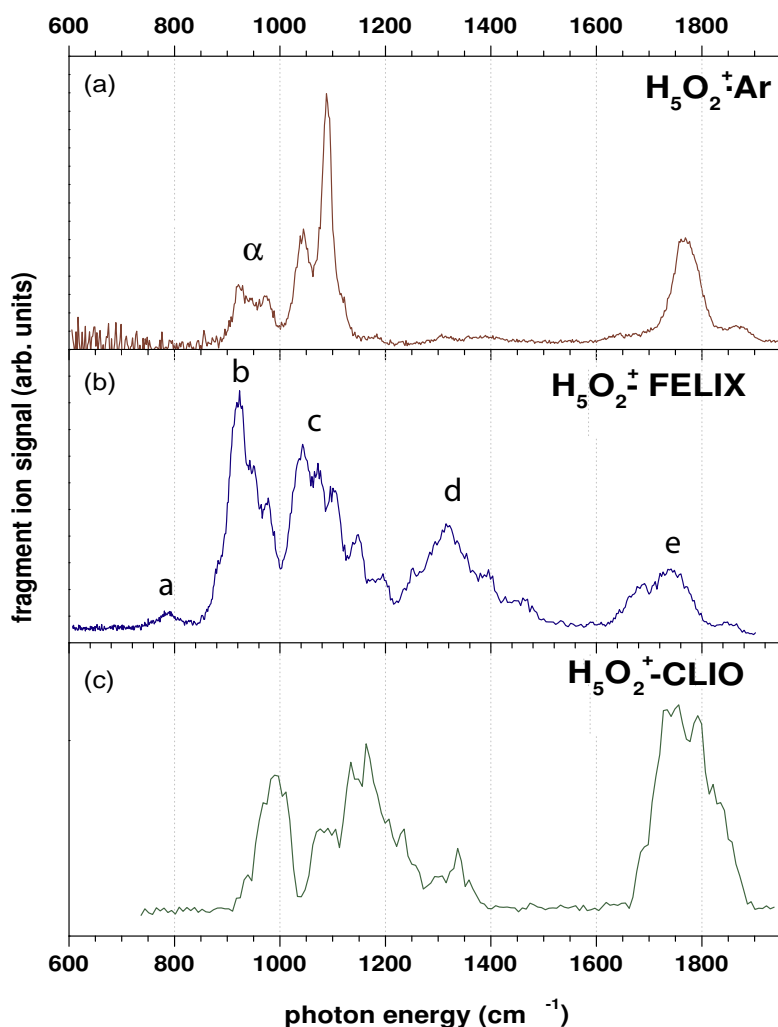


Figure 5.3: VPD spectrum of $H_5O_2^+ \cdot Ar$ ^{97,98} (a)) and IRMPD spectra of $H_5O_2^+$ measured at FELIX¹⁰⁰ (b)) and at CLIO⁹⁶ (c))

The predissociation spectrum of the Ar complex^{97,98} measured from 600 to 1900 cm^{-1} (see Figure 5.3, upper trace) presents four main peaks at 949, 1045, 1085 and 1770 cm^{-1} with smaller widths than in the IRMPD spectra. The position of most of the bands in the $H_5O_2^+ \cdot Ar$ spectrum agrees well with the position of the bands in the spectrum measured at FELIX. Discrepancies are observed for the band c of

the FELIX spectrum (with the maximum at 1043 cm^{-1}) which in the *Ar* complex is split into two bands at 1043 and 1085 cm^{-1} and for band *d* which is only very weakly observed in the VPD spectrum. Both CLIO⁹⁶ and FELIX¹⁰⁰ spectra reveal a band at the position of band *d*, with the peak in the spectrum measured at CLIO having a lower intensity. Thus, band *d*, seems to be a specific feature of the multiphoton dissociation experiment. The most intense bands in the VPD spectrum are centered at 1085 and 1770 cm^{-1} . These were assigned to the asymmetric stretch of the central proton and to the asymmetric bending vibrations of the terminal water molecules.^{97,98} The broad feature at lower energies, labeled α and centered at 949 cm^{-1} is strongly dependent on the number of attached *Ar* atoms and its origin could not be explained. No explanation was given to the band at 1045 cm^{-1} either.

It is interesting to look also at the influence of the *Ar* atom on $H_5O_2^+$. Experiments performed on the $H_5O_2^+ \cdot H_2$ cation¹⁰⁴ showed that the attachment of one H_2 molecule with a binding energy smaller than 4 kcal/mol (0.17 eV) is enough to disturb the symmetry of the hydrogen bond stabilizing a $H_3O^+ \cdots H_2O$ type complex. Headrick *et al.*⁹⁸ argued that the attachment of one *Ar* atom, does not break the symmetry of the system to form $H_3O^+ \cdots H_2O$ and only leads to a shift of the IR bands. A strong structural change should display a different spectrum than the one observed which is similar to the IRMPD spectrum of the bare ion $H_5O_2^+$. Headrick *et al.*⁹⁸ compared the position of the bands upon the attachment of one and two *Ar* atoms and assuming an additive argon perturbation, they showed that the band at 1085 cm^{-1} in $H_5O_2^+ \cdot Ar$ (located at 1140 cm^{-1} in $H_5O_2^+ \cdot Ar_2$) is placed close to the maximum of band *c* in the bare ion spectrum.

Table 5.3: Experimental vibrational frequencies determined from IRMPD spectra of the $H_5O_2^+$ cation measured at the FELIX and CLIO facilities, as well as from the VPD spectrum of the $H_5O_2^+ \cdot Ar$ complex.

$H_5O_2^+$ FELIX ^a	$H_5O_2^+$ CLIO ^b	$H_5O_2^+ \cdot Ar$ ^c
cm^{-1}	cm^{-1}	cm^{-1}
921	990	949
1043	1153	1045
		1085
1317	1340	
1741	1770	1770

^a - Reference;¹⁰⁰ ^b - Reference;⁹⁶ ^c - Reference^{97,98}

Based on the comparison of the VPD and FELIX IRMPD spectra, a different assignment than the one based on full dimensional calculations for the IRMPD spec-

trum presented here can be made. Thus, band *e* can be assigned to the asymmetric bending motion of the water monomers as discussed previously. Band *d* seems to be specific to the multiphoton experiments and hence, its assignment to a fundamental transition is questionable. Thus, bands *b* and *c* are probably involving the asymmetric and the bending vibrations of the central proton. Based on its high intensity Headrick *et al.*⁹⁸ assigned the band at 1085 cm^{-1} , which is close to band *c* in the FELIX IRMPD spectrum, to the asymmetric stretching vibration of the central proton and not band *b* as predicted by the calculations. Thus, band *b* could then be tentatively assigned to the bending motion of the central proton. The bending motion was not assigned in the VPD spectrum. The band labeled α positioned at 949 cm^{-1} in the VPD spectrum is close to band *b* located at 921 cm^{-1} in the IRMPD spectrum and thus, this band might be due to the bending vibration of the central proton. Its low intensity might be caused by the low intensity of the table-top laser used in the VPD experiments⁹⁸ at this frequency.

Based on the presented tentative assignment on $H_5O_2^+$, the bands in $D_5O_2^+$ can be assigned considering the isotope shifts. The 15D VCI calculations¹¹¹ predict an isotope shift of the asymmetric stretch higher than the harmonic value in good agreement with the 4D simulations of Vener *et al.*¹⁰⁹ However, all shifts observed in the experiment are lower than 1.37 (see Table 5.1). Based on these reasonable shifts, band *b'* at 697 cm^{-1} in $D_5O_2^+$ can be tentatively attributed to the $O\cdots D^+\cdots O$ bending vibration and band *c'* to the $O\cdots D^+\cdots O$ asymmetric stretch. Band *e'* is assigned similar as for $H_5O_2^+$ to the asymmetric bending mode of the outer D_2O monomers.

A tentative assignment can also be given to the peaks in the spectra of $D_xH_{5-x}O_2^+$. The band at 1500 cm^{-1} which appears only in the mixed spectra could be assigned to the bending motion of the *HDO* monomer. This bend is red shifted from the peak *e* in the $H_5O_2^+$ spectrum by $\approx 241\text{ cm}^{-1}$ (shift factor of 1.16). The band at 770 cm^{-1} in the $DH_4O_2^+$ can be tentatively attributed to the bending vibration of the $H_2O\cdots D^+\cdots OH_2$ isomer which is red shifted by 151 cm^{-1} from band *b* (shift factor of 1.2) in Figure 5.1. This band grows in intensity and is further red shifted (to 700 cm^{-1} for $D_2O\cdots D^+\cdots OD_2$) as the deuteration degree increases. The observed red shift suggests a coupling of this mode with the modes of the terminal water monomers. The assignment of the bands in the central region of the mixed spectra is difficult and requires theoretical support.

Conclusions

The IRMPD spectrum of the Zundel cation $H_5O_2^+$ was measured for the first time between 600 and 1900 cm^{-1} which is the region of the central proton stretches. Additionally, the IR spectra of the partially and totally deuterated cations was measured as well. The spectra are complex and reveal broad bands caused by strong mode mixing. The experimental results are compared with more recent IRMPD⁹⁶ and VPD^{97,98} measurements as well as to full-dimensional calculations. Based on the comparison with the VPD experiments a tentative assignment of the bands in $H_5O_2^+$ was presented here. Thus, band *e* was assigned to the asymmetric bending motion of the outer water monomers and bands *b* and *c* were assigned to the bending and the asymmetric stretching vibrations of the central proton. The experiments and the theory do not agree on the assignment of the bands observed in the IRMPD spectrum. Calculations that address directly the experiments that use either the *Ar* messenger atom technique or the multiphoton photodissociation techniques would offer a more insight in the IR spectrum of the Zundel cation.

5.1.3 $H_3O^+(H_2O)_3$

As discussed in the introductory Chapter 1, two limiting structures were predicted to play an important role in the proton transfer process in liquid water, namely $H_5O_2^+$ and $H_9O_4^+$. The quasi-continuum absorption characteristic for the hydrated protons in liquid water makes the assignment of specific bands to the Eigen (H_3O^+) and to the Zundel ($H_5O_2^+$) ion cores difficult. Hence, measurement of these ions in the gas phase, without the influence of the environment will offer important information.

The IR spectrum of $H_9O_4^+$ was previously measured by Lee *et al.*^{104,115} in the region of the *O – H* stretch, above 3500 cm^{-1} . The multiphoton dissociation and the messenger atom techniques were used, where for the latter, one H_2 molecule or one *Ne* atom were attached as *messenger ligands* to the chromophore. Similar to the case of the Zundel cation, the H_2 attachment disturbs the symmetry of the ion, which was evidenced in the IR spectrum by a splitting of the *O – H* stretching bands. Lee *et al.*^{104,115} observed also that the influence of the H_2 messenger atom decreases from $H_5O_2^+$ to $H_9O_4^+$. The attachment of one *Ne* atom perturbs less the hydrogen bond and induces only slight shifts of the bands on the order of 8 cm^{-1} . The IR spectrum of $H_9O_4^+$ was also measured by Schwarz *et al.*¹¹⁶ in the region from 2000 to 4000 cm^{-1} with a resolution of 40 cm^{-1} . The experiment revealed four bands in this frequency region which were assigned to the *O – H* asymmetric (3710 cm^{-1}) and

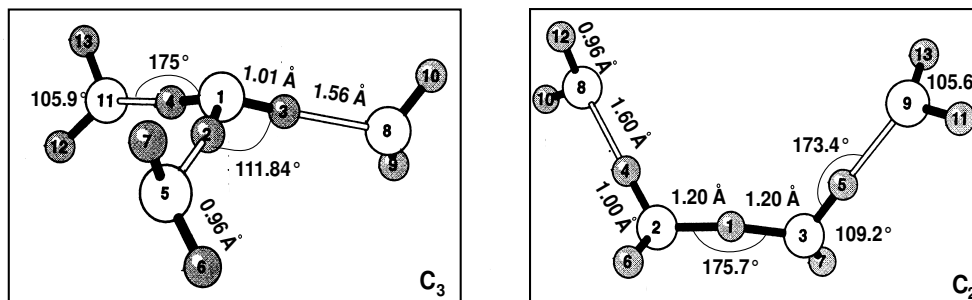


Figure 5.4: The structures of the $H_9O_4^+$ cation predicted by Ojamäe *et al.*¹⁰⁷ at the MP2/TZ2P level of theory. Oxygen atoms are displayed by dark spheres; hydrogen atoms by white spheres.

symmetric (3620 cm^{-1}) modes of the three outer water molecules and to the $O-H$ symmetric (3000 cm^{-1}) and asymmetric (2600 cm^{-1}) modes of the central H_3O^+ . These results are in good agreement with the experiments performed by Lee *et al.*¹⁰⁴ above 3500 cm^{-1} (3645 and 3730 cm^{-1} for the symmetric and asymmetric modes of the outer water molecules).

Low level calculations^{117,118} predict two minimum geometries with C_{3v} and D_{3h} symmetry, which are very close in energy. More recent calculations^{113,119,120} predict also two minimum geometries but with C_3 and C_2 symmetry (see Figure 5.4). The second geometry represents a local minimum (C_2 symmetry), higher in energy with 10.6 kJ/mol (0.11 eV). This energy was calculated using the OSS3 potential energy surface.¹²⁰ The global minimum geometry C_3 can be described as three water molecules that are hydrogen bonded to a hydronium ion H_3O^+ (see Figure 5.4, left panel). The addition of two H_2O molecules to $H_5O_2^+$ completes the first solvation shell of the H_3O^+ core. The C_2 geometry can be rather described by two water molecules bound to a central $H_5O_2^+$ unit (see Figure 5.4, right panel).

Since the structures are different, the infrared spectra of the two geometries are expected to be different as well, especially in the region below 2000 cm^{-1} where the central proton stretches occur. The IR spectra for $H_9O_4^+$ were simulated based on harmonic¹¹³ as well as quantum dynamical calculations.¹²¹ These calculations support the prediction of different spectra for the C_2 and C_3 geometries, especially below 2000 cm^{-1} (see Figure 5.5). Hence, measurements of the IR spectra of $H_9O_4^+$ in this region should reveal which one of the two isomers is present in the gas phase.

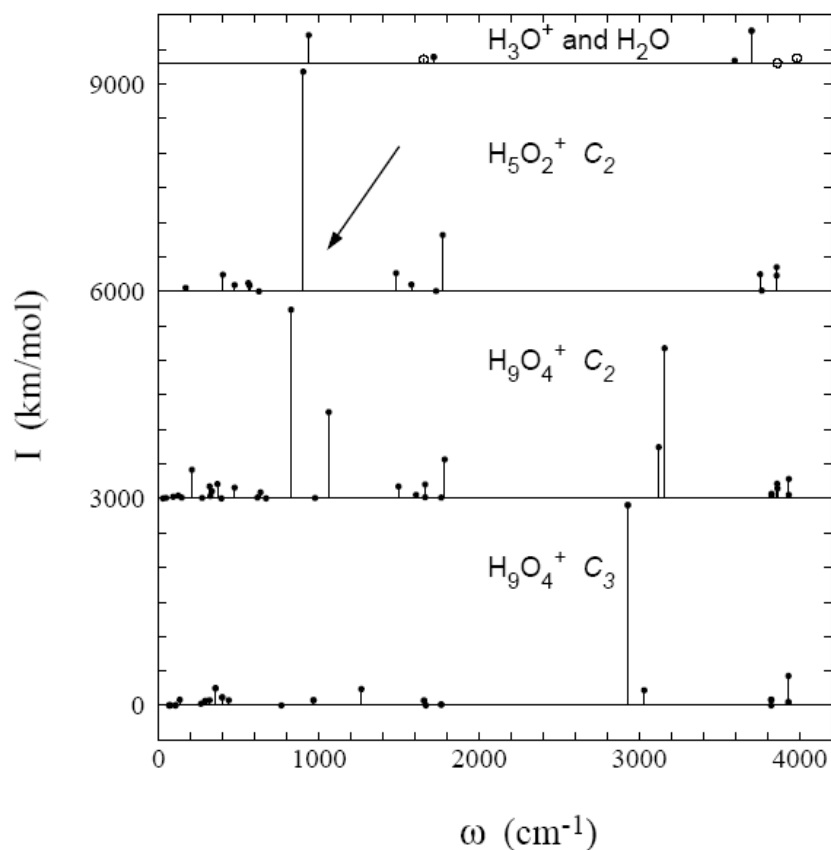


Figure 5.5: The harmonic vibrational spectra for the monomers H_3O^+ and H_2O , for $H_5O_2^+$ in C_2 symmetry and for $H_9O_4^+$ in C_2 and C_3 symmetries (MP2(TZ2P) calculations). The water monomers peaks are displayed using open circles, the others by small filled circles. The arrow indicates the position of the H -bonded $O - H$ stretching peak in $H_5O_2^+$. Taken from Ojamäe *et al.*¹¹³

Results

The IRMPD spectrum of $H_9O_4^+$ was measured between 600 and 2000 cm^{-1} (16.66 to 5 μm) (see Figure 5.6). The main dissociation channel is the H_2O -loss followed by the loss of two H_2O units. The two fragmentation channels reveal identical spectra, but the bands in the $2H_2O$ -loss spectrum have much lower intensities. Thus, the IRMPD spectrum of the second dissociation channel is attributed to a sequential dissociation process which produces $H_5O_2^+$. The IR spectrum of $H_9O_4^+$ was recorded with 0.02 μm step and a FELIX pulse energy of 28 $mJ/macropulse$ measured at 15 μm . A background signal of approximately 250 *counts/s* is produced by CID in the trap. The spectrum reveals two intense, broad bands. The first band ranges from

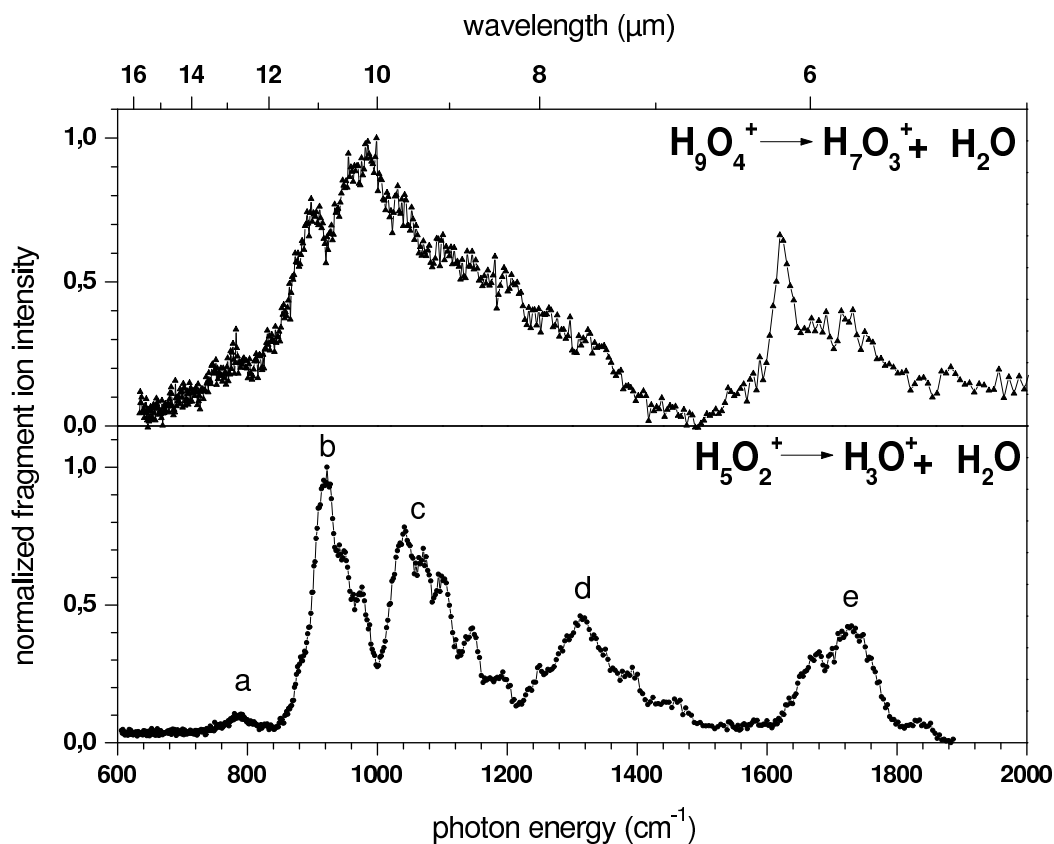


Figure 5.6: IRMPD spectrum of the $H_9O_4^+$ (upper trace, triangles) measured at FELIX energy of 28 mJ/macropulse at $15 \mu\text{m}$. The lower trace (closed circles) shows for comparison the IRMPD of the Zundel cation $H_5O_2^+$.¹⁰⁰

approximately 600 to 1450 cm^{-1} , where a shoulder centered at 900 cm^{-1} indicates the presence of an additional band. The form of the band in the high energy region suggests the presence of additional unresolved peaks. The region between 600 and 1500 cm^{-1} was recorded also at higher laser pulse energies, namely 60 mJ/macropulse measured at $15 \mu\text{m}$ (see Figure 5.7) with a step size of $0.04 \mu\text{m}$. At this pulse energy additional bands are observed which are centered at 630 , 707 and 762 cm^{-1} . The maximum of the broad band is red shifted from 976 cm^{-1} in the low pulse energy spectrum to 905 cm^{-1} in the high pulse energy spectrum. This strong laser intensity dependence suggests that the new appeared bands might arise from multiple photon transitions. In the high energy part of the spectrum shown in Figure 5.6, a second broad band with an sharp peak at 1625 cm^{-1} is observed. The high energy tail of this peak might cover at least two unresolved bands centered at 1675 and 1725 cm^{-1} .

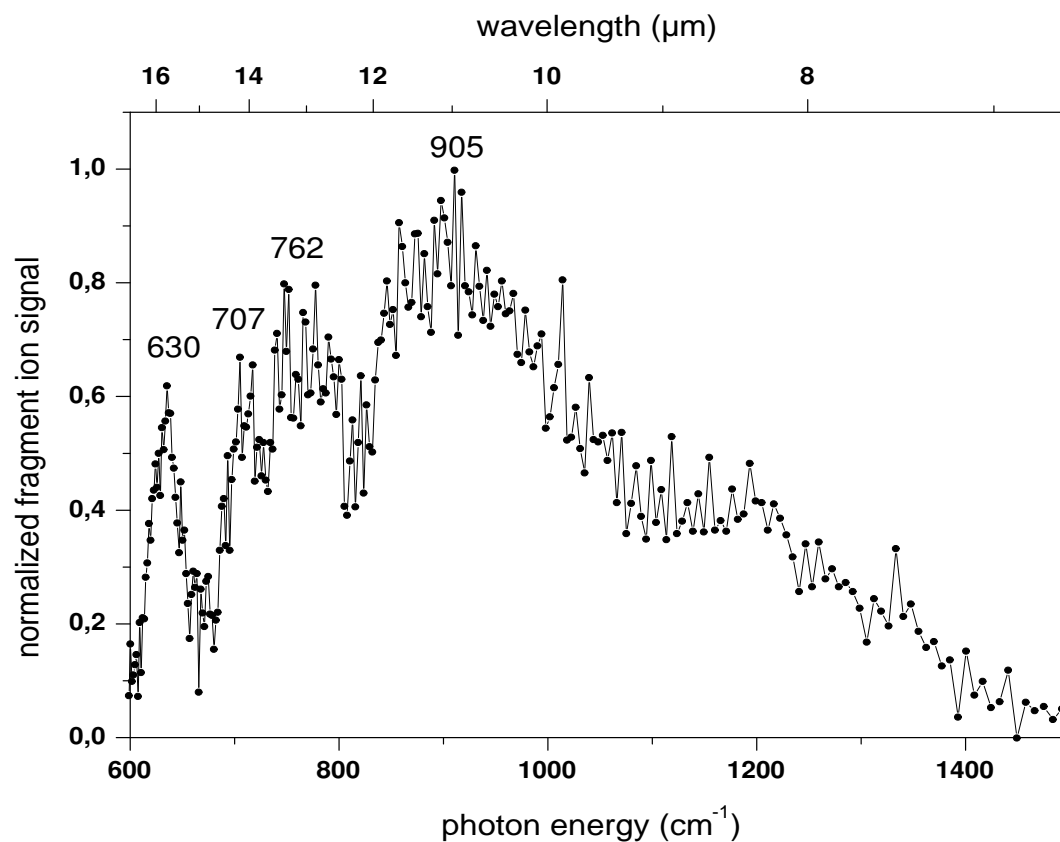


Figure 5.7: IRMPD spectrum of $H_9O_4^+$ measured at FELIX pulse energy of 60 $mJ/macropulse$ at 15 μm .

Discussions

Since the bands in the IRMPD spectra of $H_9O_4^+$ are not well resolved, the assignment of the bands to specific vibrational modes is difficult. It is, however, interesting that $H_9O_4^+$ shows strong infrared activity in the low energy region where only few low intensity peaks are predicted by the harmonic calculations for the lowest energetically lying isomer (C_3 symmetry) (see Figure 5.5, lower panel). Figure 5.6 shows the IRMPD spectra of both $H_9O_4^+$ and $H_5O_2^+$. Surprisingly, strong similarities are observed. The second band in $H_9O_4^+$, centered at 1690 cm^{-1} agrees well with band *e* in the spectrum of the Zundel cation $H_5O_2^+$ (see Figure 5.6). The first broad band seems to cover all the bands *b*, *c*, and *d*. The similarity of the two spectra suggests that the $H_9O_4^+$ isomer with the C_2 symmetry structure is the absorbing specie. Based on this similarity a tentative assignment to some of the features observed in the measured IRMPD spectrum of $H_9O_4^+$ can be proposed. Thus, the sharp feature centered at 1625 cm^{-1} is close to the bending vibrations of the free H_2O ¹²² and can be tentatively assigned to the asymmetric bending vibration of the outer water monomers

in $H_9O_4^+$. The broad band in $H_9O_4^+$ might include the bands b , c and d of $H_5O_2^+$, hence, vibrations of the central proton in a C_2 symmetry structure.

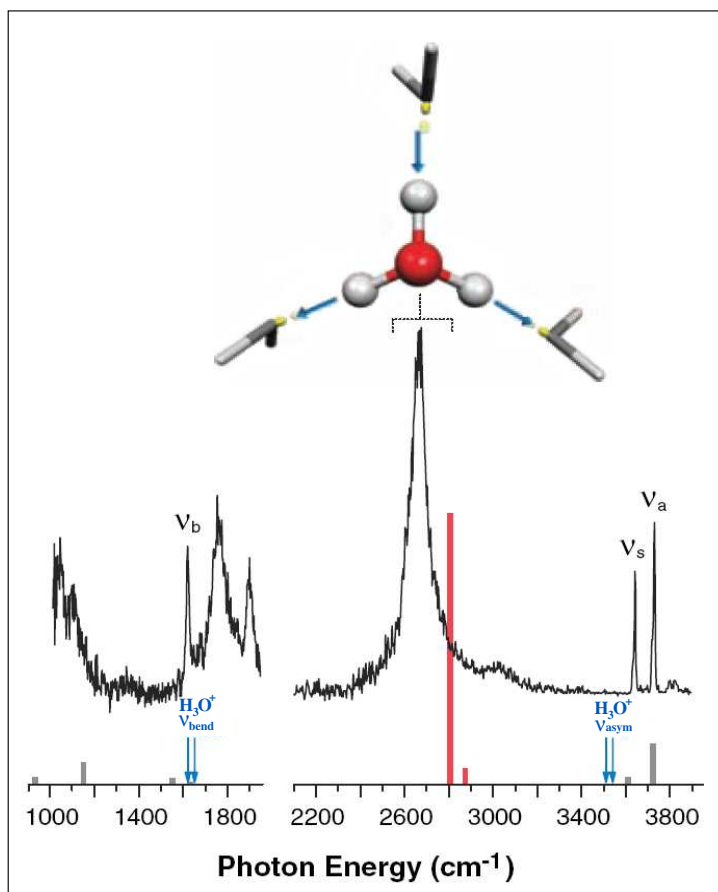


Figure 5.8: The VPD spectrum of $H_9O_4^+$. The OH asymmetric stretch (ν_{asym}) and asymmetric bending (ν_{bend}) bands of bare H_3O^+ are denoted by arrows and the MP2/aug-cc-pVDZ harmonic spectrum (0.955 scaling) is displayed by bars. The Eigen core stretches are highlighted in red. The sharp bands above 3400 cm^{-1} arise from the symmetric ν_s and asymmetric ν_a OH stretches of the water monomers with their associated intramolecular bending transitions (ν_b) at $\approx 1600\text{ cm}^{-1}$. Taken from Headrick *et al.*¹²³

Recently, Headrick *et al.* performed measurements of the IR spectrum of $H_9O_4^+$ over an extended frequency window, 1000 to 4000 cm^{-1} , using the VPD technique¹²³ (see Figure 5.8). This spectrum shows also absorptions in the low energy region, in very good agreement with the IRMPD spectrum. The VPD spectrum reveals bands at 1045 , 1620 , 1760 and 1900 cm^{-1} , which are close to the peaks at 976 , 1675 and 1725 of the IRMPD spectrum. No band was observed in the IRMPD spectrum at 1900 cm^{-1} , however this might be due to the low transmission efficiency of the $ZnSe$ optics as well as the low radiation transmission efficiency at this energy (see Appendix B).

Table 5.4: Tentative assignments and experimental vibrational frequencies determined from IRMPD spectra of $H_5O_2^+$ and $H_9O_4^+$ and VPD spectrum of $H_9O_4^+$.¹²³

Peak label in $H_5O_2^+$ spectrum	$H_5O_2^+$ cm^{-1}	$H_9O_4^+$ cm^{-1}	VPD ¹²³ cm^{-1}	Tentative assignment
		630		
		707		
<i>a</i>	788	762		
<i>b</i>	921	900		ν_8
<i>c</i>	1043	976		ν_7
			1045	$H_3O^+_{ax}$
<i>d</i>	1317	1450		
		1625	1620	ν_{11}
		1675		
<i>e</i>	1741	1725	1760	$H_3O^+_{eq}$
			2665	$H_3O^+_{as}$
			3644	H_2O symmetric stretch
			3730	H_2O asymmetric stretch

ν_7, ν_8, ν_{11} - asymmetric and bending motion of the central H -atom modes in a C_2 symmetry isomer and the asymmetric bending mode of the outer water molecules.

$H_3O^+_{ax,eq}$ - axial and equatorial bending vibrations of the solvated H_3O^+ ion.

The bands in the low energy region were tentatively assigned by Headrick *et al.*¹²³ to the symmetric bending motion of the H_3O^+ ion core along its principal axis (1045 cm^{-1}) and to bending motions in the solvated H_3O^+ ion core (1760 and 1900 cm^{-1}). The last two bands were not predicted by the harmonic calculations. The tentative assignment of these two bands was based on the frequencies which are close to the equatorial bends in the isolated H_3O^+ ion (see blue arrows labeled as $H_3O^+ \nu_{bend}$ in Figure 5.8). The band at 1620 cm^{-1} was assigned identical as in the IRMPD spectrum to the asymmetric bending motions of the water monomers. This peak is red shifted from band *e* in $H_5O_2^+$ assigned to the same vibration (see Figure 5.6, lower panel). The shift might be caused by the presence of the additional water molecules which weaken and distort the H -bond and thus, the vibrations of the water molecules become closer to the ones of free H_2O . This is supported by the dissociation energy of $H_9O_4^+$ of 75 kJ/mol^{124} (0.77 eV) which is lower than the dissociation energy of the Zundel cation of 1.37 eV^{112} . From the comparison of the VPD, harmonic

calculations and IRMPD spectra, the broad band at 976 and the band at 1725 cm^{-1} in the IRMPD spectrum can be assigned similar as in the VPD spectrum (Figure 5.8) to bending vibrations of the Eigen core. This tentative assignment together with the experimental IRMPD frequencies is listed in Table 5.4.

Although the dissociation energy of this ion is lower than for the Zundel cation, still at least four to twelve photons are required in the IRMPD spectrum for the photodissociation of $H_9O_4^+$ in the frequency window scanned by the experiment. It is possible that the multiphoton process which is involved in the experiments leads to the appearance of additional peaks, e.g., two photon absorptions which are resonant with one vibrational transition. These transitions would be observed at frequencies close to the fundamental band, but shifted due to the anharmonicity. This would lead to an increased number of closely spaced peaks which could be observed in the IRMPD spectrum, explaining the broad features which were observed in the experiment.

The VPD experiments show a strong absorption at 2665 cm^{-1} as well,¹²³ which matches the experimentally¹¹⁶ measured and theoretically¹²³ predicted degenerate asymmetric *OH* stretching vibration of the Eigen core. This peak is the signature band of $H_9O_4^+$, the Eigen-core isomer. Thus, the experiments support the C_3 symmetry structure for $H_9O_4^+$. The band at 2665 cm^{-1} shows a strong red shift (860 cm^{-1}) from the *OH* stretching motion of the isolated H_3O^+ ion (see Figure 5.8, blue arrows labeled $H_3O^+ \nu_{asym}$) caused by the hydrogen bonds which are formed by solvation. However, the observation of the low energy peaks in $H_9O_4^+$ at positions similar to $H_5O_2^+$ indicates that the spectral complexity of $H_9O_4^+$ requires theoretical investigations beyond the harmonic approximation.

Conclusions

The IRMPD spectrum of $H_9O_4^+$ was measured for the first time between 600 and 2000 cm^{-1} . The spectrum reveals very broad features in this frequency domain. Comparison of the IRMPD spectrum of $H_9O_4^+$ to the IRMPD spectrum of the Zundel cation shows strong similarities which suggest similar structures. More information is obtained from the comparison of the measured spectra with the VPD spectra of Headrick *et al.*¹²³ which extends up to 4000 cm^{-1} . This spectrum is similar in the low energy region with the IRMPD spectrum presented here. In the high energy region, however, a peak at 2665 cm^{-1} is observed which is the signature band for the Eigen-core specie, supporting the energetically lowest lying isomer as the absorbing system. The understanding of the origin of the bands in the low energy region requires additional investigations. As already mentioned by Headrick *et al.*,¹²³ calculations

beyond the harmonic approximation are required.

5.1.4 $\text{H}_3\text{O}^+(\text{H}_2\text{O})_2$

A large number of theoretical and experimental studies were performed on the Zundel cation. However, there are only few studies on $H_7O_3^+$. Calculations performed at different levels of theory^{118–120,125} predict a C_s (see inset Figure 5.9) symmetry for the $H_7O_3^+$ ion as global minimum. A C_{2v} transition state geometry is predicted to lie 2.9 *kJ/mol* (0.03 *eV*) (B3LYP/T(O)DZP value^c) higher in energy.¹²⁵ Lower level calculations¹¹⁷ predict this geometry as a local minimum. The multiphoton photodissociation and the messenger atom technique spectra of this cation were measured at energies above 3550 cm^{-1} by Yeh *et al.*¹⁰⁴ Based on SCF/DZP calculations,¹¹⁷ Yeh *et al.*¹⁰⁴ assigned the IR spectrum of $H_7O_3^+$ to the C_{2v} geometry.

Results and Discussions

In Figure 5.9, the IRMPD spectrum of $H_7O_3^+$ in the region from 600 to 2000 cm^{-1} is presented. The spectrum was measured at two different laser adjustments: a) higher intensity above 800 cm^{-1} (see Figure 5.9, middle trace) and b) higher intensity below 800 cm^{-1} (see Figure 5.9, upper trace). The spectra reveal a strong laser intensity dependence, suggesting multiple photon behavior as in the case of $H_9O_4^+$, especially in the low energy part of the spectrum. The main dissociation channel is the loss of one H_2O unit. A second dissociation channel, namely the loss of a second water molecule, is observed as well. The IR spectrum of $H_7O_3^+$ (see Figure 5.9) reveals four broad bands labeled from *A* to *D*. The first peak, *A*, with the maximum at 687 cm^{-1} has two shoulders that indicate additional bands centered at 753 and 808 cm^{-1} . The other three bands *B*, *C*, *D* have maxima at 1074, 1496 and 1851 cm^{-1} . Peak *D* shows a shoulder at 1651 cm^{-1} , which indicates an additional band. The lower trace of Figure 5.9 shows the $H_5O_2^+$ IRMPD spectrum as well. A good overlap is observed between peak *B* at 1074 cm^{-1} in the $H_7O_3^+$ spectrum and peak *c* (1043 cm^{-1}) of $H_5O_2^+$ (see Figure 5.1). Peak *c* in $H_5O_2^+$ was attributed to a vibration involving the central proton. Similar to $H_9O_4^+$, band *B* could be tentatively assigned to the symmetric bending vibration of the H_3O^+ core along its principal axis. The broad bands *A* and *D* in $H_7O_3^+$ overlap also with the bands *a* and *e* of $H_5O_2^+$, however not at the maximum. Band *e* at 1741 cm^{-1} in $H_5O_2^+$ was assigned to the bending vibration of the water monomers. Thus, the shoulder of band *D* at 1651 cm^{-1} can be

^cT(O)DZP - DZP basis set for the *H* atoms and TZP for *O*.

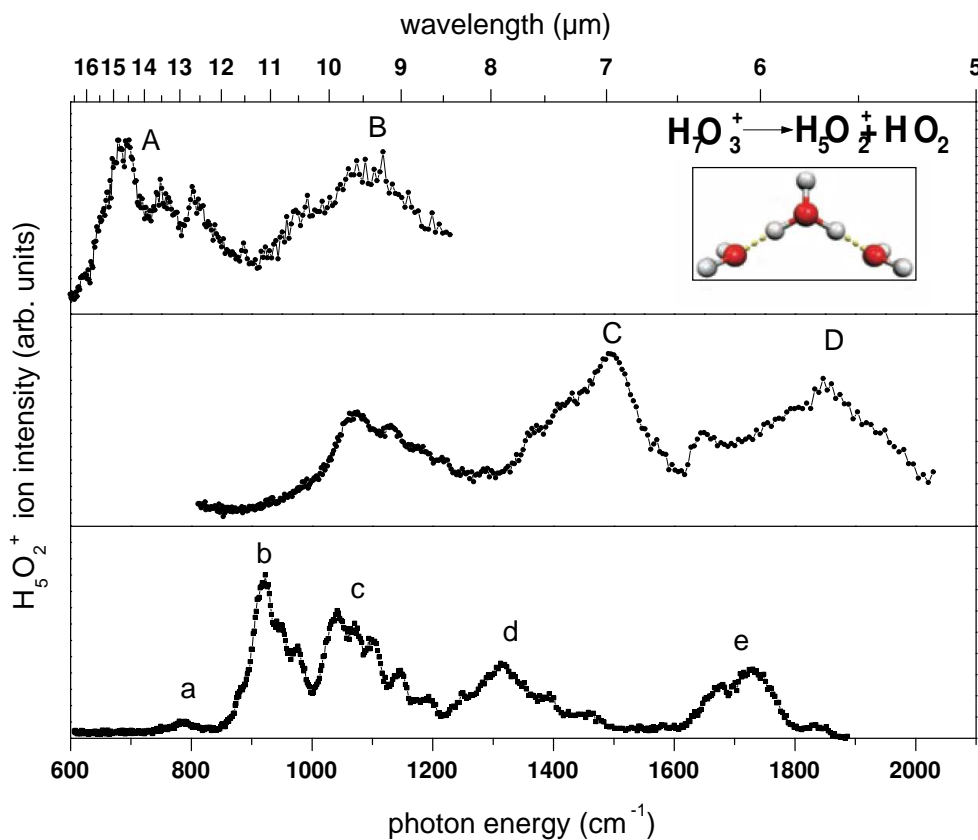
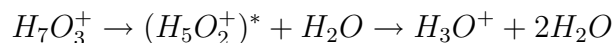


Figure 5.9: IRMPD spectrum of the $H_7O_3^+$ cation. The upper trace shows the spectrum in the low energy region (pulse energy of 44 mJ/macropulse at 910 cm^{-1}) and the middle trace in the high energy region (pulse energy of 36 mJ/macropulse at 910 cm^{-1}). The lower panel shows the IRMPD spectrum of $H_5O_2^+$. The inset shows the geometry of $H_7O_3^+$ (O - red spheres, H - white spheres.) (Inset taken from Headrick *et al.*¹²³).

assigned to the same vibration. This band is red shifted from band *e* in the Zundel cation spectrum, but blue shifted from the same vibration in $H_9O_4^+$. Band *a* at 788 cm^{-1} in the $H_5O_2^+$ spectrum has a very low intensity relative to the other bands, which is not the case for band *A* in $H_7O_3^+$. This might be due to the adjustment of the laser, which for $H_7O_3^+$ had a pulse energy of 54 mJ/macropulse in this region higher than the 40 mJ/macropulse for $H_5O_2^+$, suggesting a possible multiple photon (two photon) transition for this low energy band. The band *C* might involve bending vibrations of the solvated hydrogen atoms which are close to the predicted equatorial bending frequencies for isolated H_3O^+ (see Figure 5.8, blue arrows labeled as $H_3O^+ \nu_{bend}$). The $2H_2O$ -loss IR spectrum presents the same absorption peaks as the H_2O -loss spectrum, but with lower intensities and thus, this spectrum is attributed to

sequential dissociation.



The VPD spectrum of this cation was also recently measured with the messenger atom technique between 1000 and 4000 cm^{-1} .¹²³ The VPD spectrum indicates the absence of the 2665 cm^{-1} signature band of the Eigen cation (see previous discussion on the VPD spectrum of $H_9O_4^+$ as well as Figure 5.8.) Instead two bands at 1880 and 3580 cm^{-1} are observed. The first band is observed also in the IRMPD spectrum (band *D*). Based on anharmonic calculations, Headrick *et al.*¹²³ assigned the band at 1880 cm^{-1} to the asymmetric stretch of the two solvated protons, thus band *D* in the IRMPD spectrum presented here can be assigned to the same vibrational mode^d. This mode presents a shift of approximately 800 cm^{-1} from the signature band of the symmetrically solvated Eigen core positioned at 2665 cm^{-1} observed in $H_9O_4^+$. This indicates that changes in the hydration environment induces large shifts in the frequency of the characteristic bands of the Zundel or Eigen core. Furthermore, two bands at 1500 and 1600 cm^{-1} were observed in the VPD spectrum which are close to the maximum of band *C* and to the shoulder of band *D* in the IRMPD spectrum. The band at approximately 1600 cm^{-1} was assigned to the asymmetric bending motion of the water monomers as in the IRMPD spectrum. No assignment was presented for the band at 1500 cm^{-1} . Additionally, a very weak band at ≈ 1080 cm^{-1} is observed in the VPD spectrum close in position to the maximum of band *B* in the IRMPD spectrum. No assignment was given by Headrick *et al.* to this band either.¹²³ The above discussed tentative assignment is listed in Table 5.5.

The observed splitting and shift of the stretching vibrations of the Eigen core in $H_7O_3^+$ and $H_9O_4^+$ indicate that removal of one water molecule from the complete solvation shell leads to a concentration of the charge on the two shared proton. These pull the solvated water molecules closer to the Eigen core thus red shifting the *OH* stretch bands.¹²³

Conclusions

The IRMPD spectrum of $H_7O_3^+$ was measured for the first time between 600 and 2000 cm^{-1} at the FELIX facility. The spectrum reveals broad bands shifted from the bands in the $H_5O_2^+$ IRMPD spectrum. The difference of the IR spectra of $H_5O_2^+$ and $H_7O_3^+$ support the Eigen type structure of this ion. The IRMPD spectrum was

^dThe band at 3580 cm^{-1} was assigned by Headrick *et al.*¹²³ to the stretch of the unsolvated proton on the H_3O^+ core.

Table 5.5: Tentative assignment and experimental vibrational frequencies determined from IRMPD and VPD¹²³ spectra of $H_7O_3^+$.

Peak label in $H_7O_3^+$ spectrum	IRMPD cm^{-1}	VPD ¹²³ cm^{-1}	Tentative assignment
A	687		
	753		
	808		
B	1074	≈ 1080	$H_3O^+_{ax}$
C	1496	1500	$H_3O^+_{eq}$
D	1651	≈ 1620	ν_{11}
		1880	$H_3O^+_{as}$
	1851	2420	$H_3O^+_{sy}$
		3580	H_3O^+ free-OH stretch
		3639	H_2O symmetric stretch
	3724	H_2O asymmetric stretch	

ν_{11} - asymmetric bending mode of the outer water molecules

$H_3O^+_{sy,as}$ - symmetric and asymmetric stretching vibrations of the H_3O^+ ion core.

$H_3O^+_{ax,eq}$ - axial and equatorial bending vibrations of the solvated H_3O^+ ion core.

compared to the very recently measured VPD spectrum.¹²³ Although this ion has a predicted Eigen type structure, its IR spectrum does not show the signature band of the intact Eigen core at approximately 2660 cm^{-1} . Instead two bands at 1880 and 3580 cm^{-1} are observed. Anharmonic calculations are required to recover this splitting of the Eigen core feature in $H_9O_4^+$ on the removal of one water molecule.¹²³ Based on the comparison of the IRMPD spectra with the VPD spectra and with anharmonic calculations,¹²³ a tentative assignment to some of the experimentally observed features in the IRMPD spectrum was presented. Thus, band *D* at 1851 cm^{-1} can be assigned to the asymmetric stretch of the solvated protons. The shoulder of this band at 1651 cm^{-1} is assigned to the asymmetric bending motion of the water monomers. Bands *B* and *C* can be tentatively assigned to bending vibrations of the solvated H_3O^+ ion.

The experiments on protonated water clusters presented here indicate that asymmetries in the hydration structure around the H_3O^+ core result in strong size-dependent shifts of the characteristic absorptions assigned to the excess proton. This response to symmetry breaking might explain the lack of sharp features observed in the IR spectrum of the hydrated proton in the bulk.^{102, 123, 126}

5.2 Gas Phase Infrared Spectrum of the Hydroxide Monohydrate Anion $\text{HO}^-(\text{H}_2\text{O})$

The H_3O_2^- anion is a strong hydrogen bonded system with a double well minimum. As described in the introductory Chapter 1, the barrier between the two minima in this type of systems is close to the zero point energy. Due to its high dissociation energy of 1.2 eV,¹²⁷ this anion is a good model system for the study of strong low-barrier *H*-bonds.

There has been some contradiction in the literature concerning the geometry of the minimum structure of this anion.¹²⁸ Calculations at different levels of theory¹²⁸⁻¹³⁴ predicted two different structures, namely, one with a symmetric hydrogen bond of the type $[\text{HO} \cdots \text{H} \cdots \text{OH}]^-$ (C_2 symmetry) and a second one with a slightly asymmetric hydrogen bond, where the shared hydrogen is closer to one of the hydroxyl groups (C_1 symmetry). High level *ab initio* calculations concluded that the bridging hydrogen is delocalized over the two minima.^{99,133,134} Samson and Klopper¹³³ calculated the potential energy curve for the proton exchange of the H_3O_2^- anion and predicted a double minimum with a C_1 symmetry minimum structure and a C_2 symmetry transition state structure. A proton barrier of 0.9 ± 0.3 kJ/mol was predicted by coupled-cluster calculations,¹³³ considerably below the lowest vibrational level for protonic motion. The calculations of Huang *et al.*¹³⁴ predict that the shared proton is delocalized over the double-well potential and the *OH* groups become identical (see Figure 5.10). The experimentally predicted dissociation energy of this system is $D_0(\text{OH}^- \cdots \text{H}_2\text{O}) = 27.6$ kcal/mol (1.2 eV).¹²⁷ Due to this high dissociation energy most of the studies on $\text{OH}^- \cdot (\text{H}_2\text{O})_n$ were reduced to the $n \geq 4$.¹³⁵ Johnson *et al.*^{136,137} measured the infrared spectrum of the ion with $n = 1$ in the region of the *O* – *H* stretch above 3500 cm^{-1} . No measurements of the infrared spectrum in the region of the bridging hydrogen stretches were performed prior to our measurements. However, recently Dikens *et al.* measured the IR spectrum between 600 and 1900 cm^{-1} with the messenger atom technique.^{97,99} The recently measured VPD spectrum of for $\text{H}_3\text{O}_2^- \cdot \text{Ar}$ in the region from 600 to 1900 cm^{-1} is shown in Figure 5.11. The spectrum reveals four bands at 697, 940, 995 and 1090 cm^{-1} . Based on Monte Carlo simulations, these peaks were assigned to the asymmetric stretch (697 cm^{-1}) and to the bending vibrations (940 or 995 cm^{-1} and 1090 cm^{-1}) of the bridging hydrogen.

In this section, the IRMPD spectrum of $\text{HO}^-(\text{H}_2\text{O})$ in the region from 600 to 2000 cm^{-1} is presented and compared to the VPD spectrum of the $\text{H}_3\text{O}_2^- \cdot \text{Ar}$ measured by Diken *et al.*^{97,99}

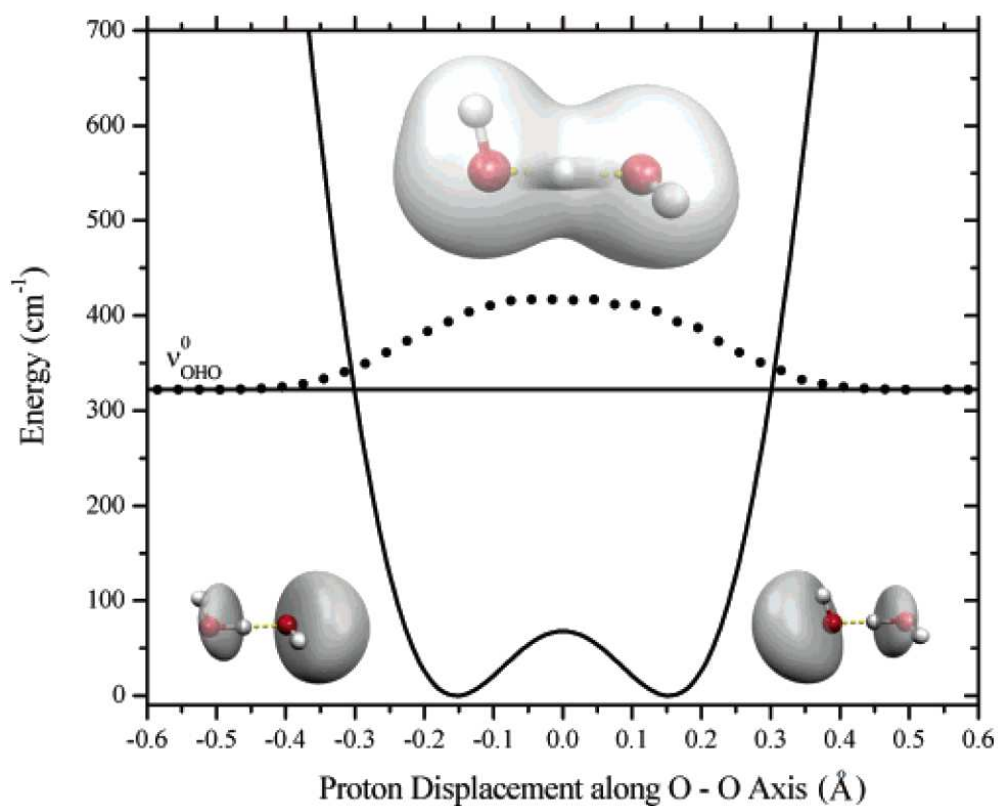


Figure 5.10: Potential energy curve of $H_3O_2^-$ along the proton displacement coordinate. The inset structures located near the bottom of the figure depict the two equivalent forms of the complex in which the shared proton is more closely associated with one of the oxygen atoms (O - red spheres, H - white spheres). The upper inset depicts the zero-point averaged structure with the proton equally shared by the two OH groups. Taken from Dicken *et al.*⁹⁹

Experiment

The $H_3O_2^-$ ions were produced by passing a gas mixture of 20% O_2 in He gas over a small amount of water vapor and expanded into the vacuum chamber through a nozzle with variable diameter between 10 and 70 μm . The ions are generated by dissociative attachment as described in Chapter 2 and are further guided to the trap, where they are collisionally thermalized in a He pressure of 0.01 *mbar* and are stored at a trap temperature of 20 *K*. The FELIX laser beam is directed into the vacuum chamber through a *ZnSe* and a *KBr* window and is focused into the ion trap by a 480 *mm KBr* lens.

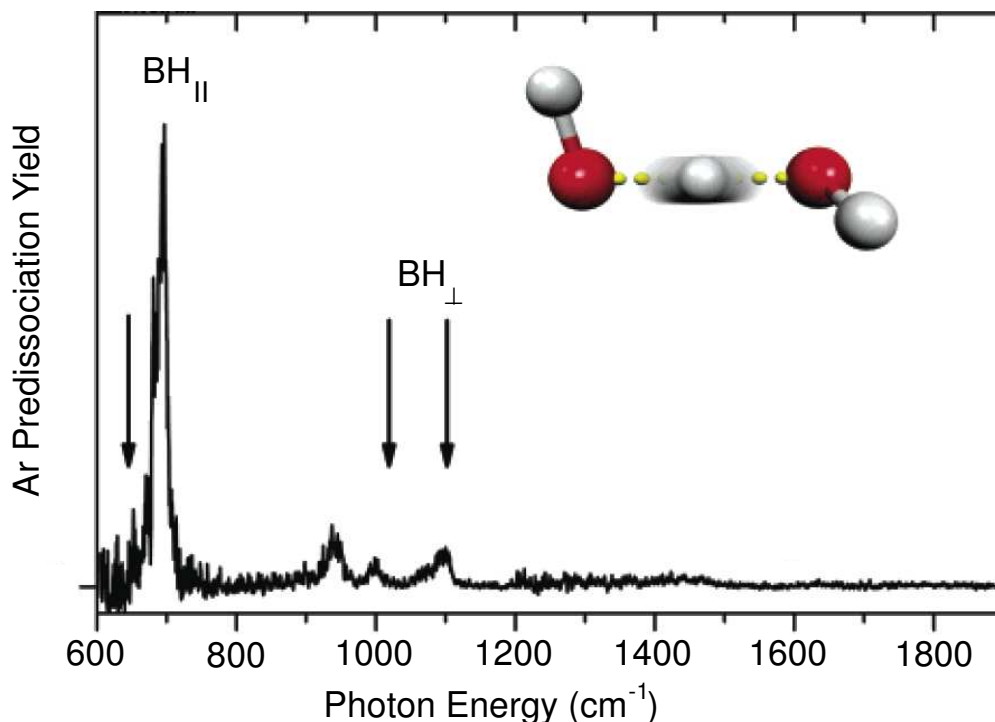
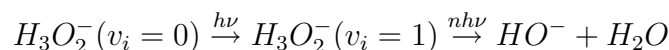


Figure 5.11: Argon predissociation spectrum of the $OH^- \cdot H_2O \cdot Ar$ complex. The dashed arrow marks the fundamental for the bending mode of the isolated water monomer. The inset shows the structure of $H_3O_2^-$ (O - red spheres, H - white spheres). Adapted from Dicken *et al.*⁹⁷

Results and Discussions

The IRMPD spectrum of $H_3O_2^-$ was measured between 600 and 2000 cm^{-1} (see Figure 5.12). As mentioned in the case of the protonated water ions, the first step in the photodissociation process between $v = 0$ and $v = 1$ is generally considered one-photonic:



However, at the laser pulse energies emitted by FELIX (≈ 60 mJ) also multiple photon transitions are possible. Considering the dissociation energy of $D_0 = 1.20$ eV (9679 cm^{-1}),¹²⁷ at least five to sixteen photons are required for dissociation in the frequency region of the experiment. The upper trace in Figure 5.12 shows the depletion spectrum of the parent ion, whereas the lower trace presents the formation of the HO^- fragment ion. A low HO^- fragment ion background signal (5 counts/s) produced through collision induced dissociation in the trap is observed. The observed peaks are labeled from A to J for the parent ion and from C' to J' for the fragment

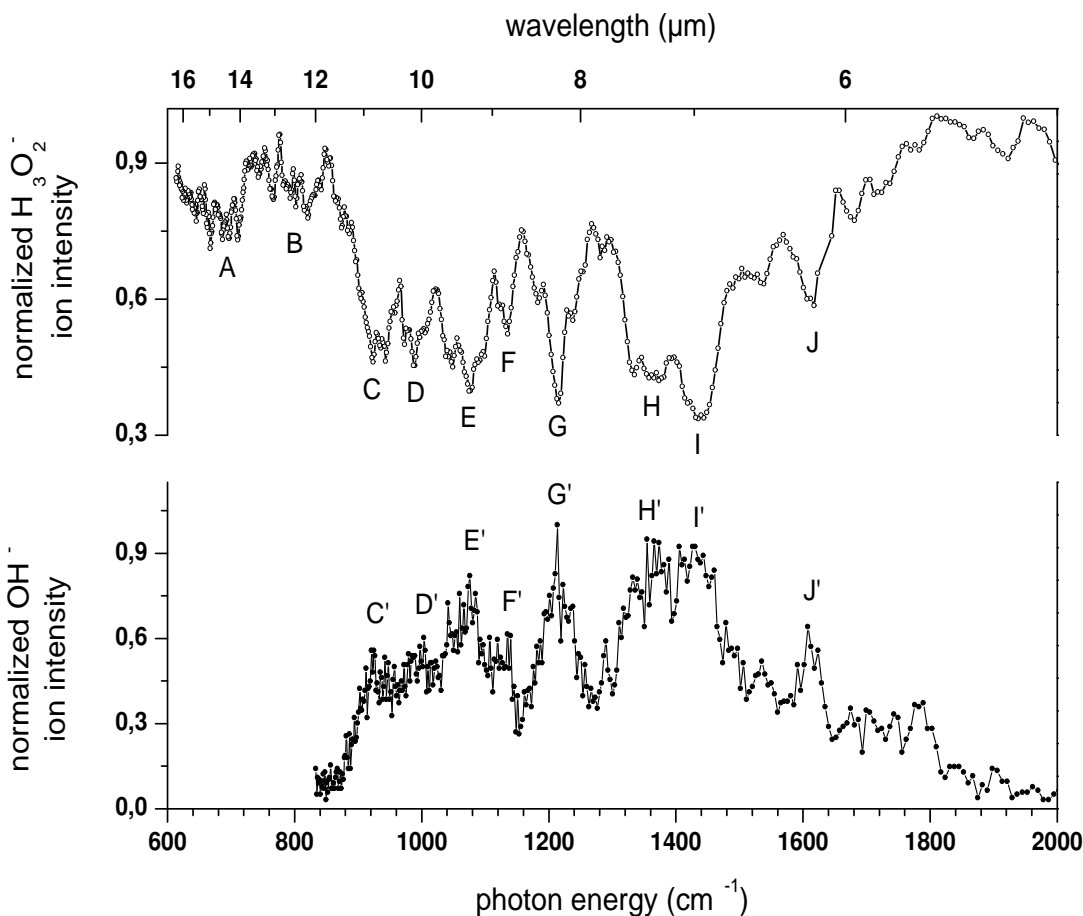


Figure 5.12: The IRMPD spectrum of $H_3O_2^-$. The upper trace presents the normalized depletion signal and the lower trace the formation of the HO^- fragment ion.

ion. The positions of the peaks are listed in Table 5.6. Peaks C , D , E , G , and H present shoulders with separations of approximately 30 and 20 cm^{-1} . The separation of the central frequencies between bands C , E and G and between D and F is approximately 140 cm^{-1} suggesting combination bands with low frequency modes.

A strong difference is observed between the IRMPD and the VPD spectra (see Figures 5.11 and 5.12), the first being more complex. The VPD spectrum reveals only four bands at 697 , 940 , 995 and 1090 cm^{-1} assigned to the asymmetric and bending vibrations of the bridging hydrogen. The simplicity of the VPD spectrum can be attributed to a lower internal energy of the Ar complexed ion. Perturbations due to the messenger atom, which might distort the symmetry of the hydrogen bond are also possible. It needs to be mentioned as well that the laser energies from the experiments performed by Diken *et al.*^{97,99} are significantly lower ($\approx 250\text{ }\mu\text{J}$ at 1500 cm^{-1}) than the energies used in the IRMPD experiments shown here ($\approx 40\text{ mJ}$ at 1500 cm^{-1}). Consequently, multiple photon transitions might occur and some of the

peaks in the IRMPD absorption spectrum of the $H_3O_2^-$ anion presented here might arise from such transitions.

All four peaks observed in the VPD spectrum of Diken *et al.*^{97,99} can be observed in the IRMPD spectrum as well and are listed in Table 5.6. However, the relative intensities are different. The VPD spectra predict the highest intensity band at 697 cm^{-1} which was also assigned by Dicken *et al.*^{97,99} to the asymmetric stretching vibration. In the IRMPD spectrum this band has a low intensity (peak A). The corresponding bands in the VPD spectrum predicted to the bending motions of the shared hydrogen ($940, 995$ and 1090 cm^{-1}) have in the IRMPD spectrum two times higher intensity than the peak at 697 cm^{-1} . This intensity difference might be due to the lower radiation transmission efficiency of the *ZnSe* window at 600 cm^{-1} compared to 1000 cm^{-1} . Additionally, at this energy a higher number of photons is required in order to reach the dissociation threshold. The Monte Carlo simulations,⁹⁷ based on which the assignment of the VPD spectrum was performed, predict the asymmetric stretch of the bridging hydrogen much lower (645 cm^{-1}) than previous calculations (819 cm^{-1} and 1028 cm^{-1}).^{133,134} Based on the comparison of the here presented IRMPD spectrum with the new experiments of Dicken *et al.*^{97,99} and on the Monte Carlo simulations a tentative assignment of the bands in Figure 5.12 is made and is listed in Table 5.6. Thus, the peak at 690 cm^{-1} is assigned to the asymmetric stretch of the bridging hydrogen. The peaks located at $937, 992$ and 1097 cm^{-1} are close to the corresponding VPD bands positioned at $940, 995$ and 1090 cm^{-1} are assigned to the two bending modes. In the VPD spectrum it could not be with certitude indicated which of the two bands at 940 or 995 cm^{-1} correspond to the bending mode. The identical intensities of the two bands in the IRMPD spectrum makes difficult the assignment of one of the two bands to the bending motion of the bridging hydrogen. Therefore, in the assignment presented here, both possibilities are considered. Huang *et al.*⁹⁹ performed full dimensional VCI calculations on $H_3O_2^-$ as well. They predict strong mode mixing of the vibrations involving the bridging hydrogen with the torsion of the *OH* groups which is predicted at 140 cm^{-1} . If this value is considered for the interpretation of the IRMPD results, the bands at $1074, 1131, 1214, 1234$ and 1367 cm^{-1} can be tentatively assigned to combination bands of the bending modes with the torsion ν_2 of the *OH* groups (see Table 5.6). The additional bands which are observed might be due to multiple photon transitions as observed in the case of the IRMPD experiments on *BrHBr*⁻ and *BrHI*⁻.

We tried also to measure the predissociation spectra of $H_3O_2^- \cdot Ar$ and $H_3O_2^- \cdot Kr$, however, the spectra revealed no IR activity. Furthermore, we tried to measure the

IRMPD spectra of the larger anions, $H_5O_3^-$ and $H_7O_4^-$. The spectra were strongly intensity dependent and measured on different days revealed different IR spectra. Hence, further experimental studies are necessary for these systems.

Conclusions

The IRMPD spectrum of the hydroxide monohydrate was measured for the first time at the FELIX facility in the region of the fundamental hydrogen atom stretches, below 2000 cm^{-1} . This anion is a good model system for the study of strong low barrier hydrogen bonds. Compared to the recently performed VPD spectra, the IRMPD spectrum is more complex. This was attributed to the lower internal energy of the *Ar* complexed ion. Based on the VPD experiments and on high level theoretical calculations, a tentative assignment of most of the bands in the IRMPD spectrum of $H_3O_2^-$ was proposed here.

Table 5.6: Peak positions, normalized intensities and tentative assignments of the IRMPD spectrum of $H_3O_2^-$. The last two columns show the results of the VPD experiments of Diken *et al.*⁹⁷

Peak label	IRMPD			VPD ^a	
	Frequency cm^{-1}	Intensity	Assignment	Frequency	Assignment cm^{-1}
A	690	0.40	ν_1	697	ν_1
B	813	0.30			
C	923	0.80			
	937	0.80	ν_{6a}^*	940	ν_{6*}
D	970	0.74			
	992	0.80	ν_{6b}^*	995	ν_{6*}
E	1044	0.80			
	1074	0.90	$\nu_{6a} + \nu_2$		
	1097	0.80	ν_7	1090	ν_{7*}
F	1131	0.70	$\nu_{6b} + \nu_2$		
G	1184	0.60			
	1214	0.94	$\nu_{6a} + 2\nu_2$		
	1234	0.67	$\nu_7 + \nu_2$		
H	1336	0.85			
	1367	0.85	$\nu_7 + 2\nu_2$		
I	1437	1.00			
J	1609	0.61			

^a From reference.⁹⁷

ν_1 , ν_6 , ν_7 are the asymmetric and the two bending modes of the bridging hydrogen and ν_2 is the torsion of the water molecules.

* - in reference⁹⁷ it is not exactly specified which of the two bands can be attributed to the bending vibration of the bridging hydrogen.

ν_{6a} , ν_{6b} represent the two bands assigned in the VPD experiments to the same bending motion and are labeled as *a* and *b* in order to facilitate further assignments of the bands in the IRMPD experiment.